Cerebral Cortex September 2015;25:2842–2853
doi:10.1093/cercor/bhu079
Advance Access publication April 25, 2014

The Effects of X Chromosome Loss on Neuroanatomical and Cognitive Phenotypes During Adolescence: a Multi-modal Structural MRI and Diffusion Tensor Imaging Study

Sheng Xie[1], Zhixin Zhang[2], Qiuling Zhao[2], Jiaying Zhang[3,4], Suyu Zhong[3,4], Yanchao Bi[3,4], Yong He[3,4], Hui Pan[5] and Gaolang Gong[3,4]

[1]Department of Radiology, [2]Department of Pediatrics, China–Japan Friendship Hospital, Beijing 100029, China, [3]State Key Laboratory of Cognitive Neuroscience and Learning & IDG/McGovern Institute for Brain Research, [4]Center for Collaboration and Innovation in Brain and Learning Sciences, Beijing Normal University, Beijing 100875, China and [5]Key Laboratory of Endocrinology, Ministry of Health, Department of Endocrinology, Peking Union Medical College Hospital, Chinese Academy of Medical Sciences, Beijing 100730, China

Address correspondence to Gaolang Gong, PhD, State Key Laboratory of Cognitive Neuroscience and Learning, Beijing Normal University, Beijing 100875, China. Email: gaolang.gong@bnu.edu.cn, gaolang.gong@gmail.com

The absence of all or part of one X chromosome in female humans causes Turner's syndrome (TS), providing a unique "knockout model" to investigate the role of the X chromosome in neuroanatomy and cognition. Previous studies have demonstrated TS-associated brain differences; however, it remains largely unknown 1) how the brain structures are affected by the type of X chromosome loss and 2) how X chromosome loss influences the brain–cognition relationship. Here, we addressed these by investigating gray matter morphology and white matter connectivity using a multimodal MRI dataset from 34 adolescent TS patients (13 mosaic and 21 nonmosaic) and 21 controls. Intriguingly, the 2 TS groups exhibited significant differences in surface area in the right angular gyrus and in white matter integrity of the left tapetum of corpus callosum; these data support a link between these brain phenotypes and the type of X chromosome loss in TS. We further showed that the X chromosome modulates specific brain–cognition relationships: thickness and surface area in multiple cortical regions are positively correlated with working-memory performance in controls but negatively in TS. These findings provide novel insights into the X chromosome effect on neuroanatomical and cognitive phenotypes and highlight the role of genetic factors in brain–cognition relationships.

Keywords: diffusion tensor imaging (DTI), gray matter morphology, magnetic resonance imaging (MRI), the X chromosome, Turner's syndrome, white matter connectivity

Introduction

The X chromosome comprises ~4% of the human genome and has long been considered to play a crucial role in the development of the human brain and intelligence (Lehrke 1972; Turner 1996; Johnson et al. 2009). X-linked gene defects have been disproportionately found in various psychiatric disorders and particularly in mental retardation (Ropers and Hamel 2005; Skuse 2005). Genomic data demonstrated that a large number of X-linked genes are involved in postsynaptic protein coding, which is essential for neuronal plasticity and cognitive processes (Laumonnier et al. 2007; Swingland et al. 2012).

In healthy women with a standard karyotype (46XX), one of the 2 copies of the X chromosome is randomly inactivated to ensure the equal expression of X-linked genes with men (46XY), although a set of genes escapes this X inactivation (Carrel et al. 1999; Disteche 1999). Additionally, to match the expression level of the X-linked genes on the single X chromosome with those of the autosomal genes on the 2 copies, the gene expression of the active copy of the X chromosome is up-regulated in human somatic tissues (Nguyen and Disteche 2006a,b). Intriguingly, this X-linked gene dosage compensation exhibited variations between tissues, leading to a higher global expression of X-linked genes in brain tissues than other tissues for both humans and mice (Nguyen and Disteche 2006a,b). The observed excess dosage in the brain further supports an essential role of the X chromosome in brain development and function. However, to date, empirical investigations on how the X chromosome influences brain structure and function remain scarce, particularly in humans.

A naturally occurring "knockout model" for studying the role of the X chromosome in human brain phenotypes is Turner's syndrome (TS), a disorder in female humans characterized by the absence of all or part of a normal second X chromosome (Sybert and McCauley 2004). TS occurs in ~1 per 2000 live female births and typically leads to aberrant physical phenotypes such as short stature and gonadal dysgenesis (Gravholt 2005). Notably, cognitive deficits in visuospatial, math, and social processing have been repeatedly reported in TS (Rovet 2004; Hong and Reiss 2012), implying TS-associated brain differences. Previous magnetic resonance imaging (MRI) studies have found neuroanatomical differences in TS patients, including the reduction of parieto-occipital gray matter (GM) volume (Reiss et al. 1995; Molko et al. 2004; Marzelli et al. 2011), as well as aberrant thickness or/and surface area in specific cortical regions (Raznahan et al. 2010; Lepage, Clouchoux et al. 2013; Lepage, Hong et al. 2013; Lepage, Mazaika, et al. 2013) and impaired white matter (WM) integrity in superior longitudinal fasciculus (Holzapfel et al. 2006; Yamagata et al. 2012).

In "classical" TS patients, the entire second X chromosome is absent in all cells; this is referred to as X-monosomy (nonmosaic TS) (Sybert and McCauley 2004). Notably, it has been recognized that a number of TS patients exhibit mosaicism that is characterized by X-monosomy and another cell line with the presence of the second X chromosome, that is, losing the entire second X chromosome in only a proportion of their cells (mosaic TS). These 2 subtypes of TS patients provide a valuable opportunity to understand the "dosage effect" of the X chromosome on neuroanatomy. It is possible that any X chromosome loss could fundamentally influence the neuroanatomy in a similar manner for both nonmosaic and mosaic cases. Alternatively, the degree of neuroanatomical changes could be a function of the type of X chromosome loss. The majority of previous studies either included only nonmosaic

patients or mixed the 2 types of TS patients. Murphy et al. (1993, 1997) did compare the 2 TS groups and showed significant between-subtype differences in the sub-cortical nuclei volume and cerebral metabolic rates. However, it remains unknown how the 2 lower-order components of cortical volume, cortical thickness and surface area, and WM connectivity may be affected by X chromosome dosage.

Additionally, while previous studies have demonstrated the impact of X chromosome loss on brain structures, the mechanisms of its role in cognition have been largely a matter of speculation based on functional localizations under normal conditions, such as linking the TS-associated volume reduction in the parieto-occipital region with deficits in visuospatial and math skills (Reiss et al. 1995; Molko et al. 2004). However, a few studies have revealed significant correlations between specific brain measures and cognitive scores within a healthy control group but not within a TS group or vice versa (Murphy et al. 1997; Lepage, Hong, et al. 2013), therefore implying a TS-associated difference in the brain–cognition relationship. Moreover, recent studies have explicitly demonstrated that brain–cognition relations can be modulated by specific genes in a healthy population (Schmidt et al. 2009). Therefore, given the loss of the X chromosome, specific relationships between the cortical morphology/WM connectivity and cognitive performance may be altered in TS patients, further underlying the TS-specific cognitive profiles.

In the current study, we examined 1) whether there is an "X chromosome dosage effect" on GM morphology and WM connectivity and 2) whether the loss of the X chromosome alters the relationship between brain structures (morphology or connectivity) and cognitions. To test these, healthy control, mosaic and nonmosaic TS patients of adolescent age were included. A set of cognitive assessments was performed, and structural MRI and diffusion tensor imaging (DTI) scans were collected to measure brain morphology and connectivity.

Method and Materials

Participants

The TS patients (34 females; age range: 9–18 years) were recruited from the China–Japan Friendship Hospital (CJFH) and Peking Union Medical College Hospital (PUMCH). Age-matched healthy controls (21 females; age range: 10–18 years) were recruited through local community and parent networks. For each patient, TS was confirmed using a standard cytogenetic karyotype assessment with peripheral blood. In the TS group, 21 had a nonmosaic 45XO karyotype; 13 patients showed mosaicism with 45XO and the other cell line with the presence of the second X chromosome. For the mosaic TS patients, the percentage of peripheral blood cells with the 45XO karyotype differed across subjects (range: 17–77%; mean: 44%; standard deviation: 18%). All of the TS patients showed defective ovarian development, which was verified via pelvic ultrasound tests. Among the TS patients, 29 (19 nonmosaic and 10 mosaic) were on growth hormone (GH) treatment and only 6 (4 nonmosaic and 2 mosaic) were on estrogen replacement (ER). All participants were screened for medical history to ensure that there was no evidence of current or past major neurological or psychiatric disorders. Additionally, there were no visible abnormalities (e.g., white matter hypointensity) on the MR images, which were examined by an experienced radiologist. For each participant, traveling and accommodation expenses for participating in this study were reimbursed. The research protocol was approved by the Research Ethics Committee of the Beijing Normal University. For each participant, informed written consent was obtained from her legal guardian.

Cognitive Assessment

For each participant, the cognitive assessments were performed within 2 days prior to or after the MRI scan. The participants aged 6–16 years were assessed with the Chinese version of Wechsler Intelligence Scale for Children-Fourth Edition (WISC-IV). A total of 5 composite scores were generated using the WISC-IV: full scale intelligence quotient (FSIQ), verbal comprehension index (VCI), perceptual reasoning index (PRI), processing speed index (PSI) and working-memory index (WMI).

Given that math deficiency has been consistently reported in TS, we further tested the participants using 3 math tasks: number comparison, numerosity comparison, and simple subtraction (Wei et al. 2012). The tasks have been programed using web-based applications (http://www.dweipsy.com/lattice/) and therefore were performed online. For each math task, we used the number of correct responses per minute as the cognitive measure.

MRI Acquisition

All MRI scans were performed on the same 3T Siemens Tim Trio MRI scanner in the Imaging Center for Brain Research, Beijing Normal University. For each participant, the head was secured using straps and foam pads to minimize head movement. High-resolution 3D T_1-weighted images were sagittally acquired using a magnetization prepared rapid gradient echo (MPRAGE) sequence: 144 sagittal slices; echo time (TE), 3.39 ms; repletion time (TR), 2530 ms; inversion time (TI), 1100 ms; 1.33-mm slice thickness with no gap; acquisition matrix, 256×256; 1×1 mm in-plane resolution; acquisition time, 8:07 min. Diffusion MRI was axially applied using a single-shot echo planar imaging-based sequence: coverage of the whole brain; 62 axial slices; TR, 8000 ms; TE, 89 ms; 30 optimal non-linear diffusion-weighted directions with $b = 1000$ s/mm^2 and one additional image without diffusion weighting (i.e., $b = 0$ s/mm^2); average, 2; 2.2-mm slice thickness; acquisition matrix, 128×128; 2.2×2.2 mm in-plane resolution; acquisition time, 9:08 min.

Image Processing

Cortical Thickness and Surface Area

Here, we used the CIVET pipeline to determine the regional thickness and area of the cortical surface, as previously described (Gong et al. 2012). Briefly, the native T_1-weighted MR images were first linearly aligned in the stereotaxic space and corrected for nonuniformity artifacts using the N3 algorithm (Sled et al. 1998). The resultant images were further segmented into gray matter, white matter, and cerebrospinal fluid (Zijdenbos et al. 2002; Tohka et al. 2004). Next, the inner and outer gray matter surfaces were automatically extracted for each hemisphere using the CLASP algorithm (MacDonald et al. 2000; Kim et al. 2005). The individual surfaces were further aligned with a surface template to enable comparisons at corresponding vertices across subjects. The cortical thickness was

measured between the 2 surfaces at 40 962 vertices per hemisphere using the linked distance in the native space (Lerch and Evans 2005). The middle cortical surface, defined at the geometric center between the inner and outer cortical surfaces, was used to calculate the cortical surface area in the native space (Lyttelton et al. 2009). According to the automated anatomical labeling (AAL) template (Tzourio-Mazoyer et al. 2002), the cortical surfaces for each hemisphere were parcellated into 39 distinct regions (Fig. 1*A*). For each cortical region, the mean thickness and total area were calculated as the morphological measures.

Volume of GM Sub-cortical Structures

We quantified the volume of the sub-cortical structures. Specifically, the FMRIB Integrated Registration and Segmentation Tool (FIRST) was employed to yield a closed mesh for each sub-cortical structure in the native space (Patenaude et al. 2011), thereby defining each structure by segmentation and enabling subsequent volume calculation. Here, a total of 14 sub-cortical structures were calculated: bilateral thalamus, caudate, putamen, pallidum, hippocampus, amygdala, and nucleus accumbens.

WM Diffusion Measures

Diffusion-weighted images were processed with the PANDA pipeline toolbox (Cui et al. 2013). Briefly, PANDA called the modules of the FMRIB Software Library (FSL) to finish the skull-stripping, simple-motion and eddy-current correction, diffusion tensor/parameter calculation, and spatial normalization (Jenkinson et al. 2012). For analysis, the 2 most commonly used diffusion parameters, fractional anisotropy (FA) and mean diffusivity (MD), were chosen (Beaulieu 2002). Here, we conducted an analysis at the regional level using the White Matter Parcellation Map (WMPM) (Mori et al. 2008). Specifically, a total of 68 WMPM regions were chosen (Fig. 1*B*), including the "core white matter" as well as the reproducible blade-type white matter structures beneath the cortical gyri (Mori et al. 2008; Oishi et al. 2008). The remaining peripheral WM regions near the cortex were excluded because they are highly variable across individuals. For each WMPM region, the mean FA and MD were calculated as the connectivity measures.

Statistical Analysis

To assess the differences between groups in age and intelligence quotient (IQ) scores, we used a general linear model (GLM) with the group (healthy control, mosaic TS, and nonmosaic TS) as a main factor. For the scores in math-related tasks, age was included as a covariate in the model. For the group effects of age and the cognitive scores, $P < 0.05$ was considered significant. If a group effect was found to be significant, post hoc pairwise comparisons were further applied with the Bonferroni correction.

For each brain measure, we first tested if there was a global effect of X chromosome loss. Specifically, a repeated-measures GLM was applied in which the group was used as a main factor and the region was treated as a repeated factor. For the main group effect, $P < 0.05$ was considered significant, indicating a global effect of X chromosome loss on the brain measure. Post hoc pairwise comparisons with the Bonferroni correction were further applied if a significant main group effect was found. In the statistical models, age was included as a covariate. Note that the interaction term "age × group" was first included but showed no significance for all measures; therefore, this term was excluded from the final model (Engqvist 2005). To control for the effect of brain size in cortical thickness, surface area, and sub-cortical volume analyses, the statistical models also included the whole-brain volume as a covariate.

We further tested the "region × group" interaction in the above repeated-measures GLM. A significant "region × group" interaction here indicates a difference of the group effect between regions, therefore implying a spatially localized effect of the X chromosome loss. In this case, to identify the localized spatial pattern of the effect, the brain measure for each region (i.e., the cortical thickness/surface area for each AAL cortical region, the volume for each sub-cortical structure, or the FA/MD for each WMPM region) were compared between groups, respectively. Likewise, age was included as a covariate in all statistical models, and the whole-brain volume was controlled when analyzing the cortical thickness, surface area, and sub-

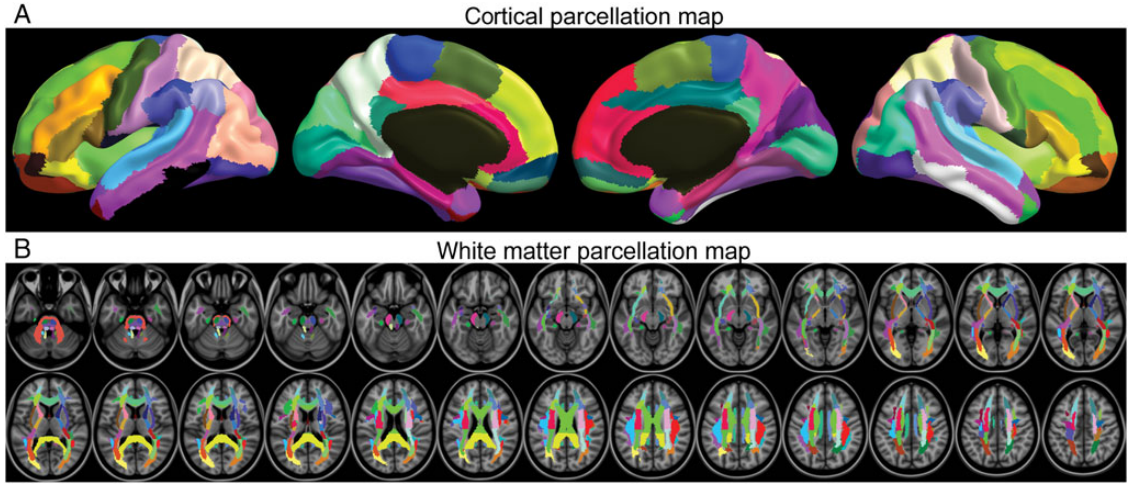

Figure 1. Regional parcellation for the cortex and white matter. (*A*) The cortical parcellation map overlaid on the average surface. This parcellation (in total 78 cortical regions) was based on the automated anatomical labeling (AAL) template. (*B*) The white matter parcellation map (WMPM) overlaid on the average T_1 image. The WMPM (in total 68 WM regions) included the "core white matter" as well as the reproducible blade-type white matter structures beneath the cortical gyri.

cortical volume. For each brain measure, the false discovery rate (FDR) procedure was performed to correct for multiple comparisons across different regions, and $q < 0.05$ (i.e., FDR corrected $P < 0.05$) was chosen as the level of significance (Genovese et al. 2002). If a region exhibited a significant main group effect (i.e., $q < 0.05$), post hoc pairwise comparisons were further applied using the Bonferroni correction.

To determine if the X chromosome modulates brain–cognition relations, we tested the "brain measure × group" interaction on each of the cognitive items. This interaction represents the group difference in the regression slopes between the brain measures (e.g., cortical thickness, surface area, sub-cortical volume, FA, or MD) and cognitions. Additionally, all statistical models included age as a covariate, and the whole-brain volume was further included as a covariate for cortical thickness, surface area, and sub-cortical volume analyses. Similarly, to correct for multiple comparisons across different regions, the FDR procedure was applied for each brain measure, and $q < 0.05$ was considered statistically significant.

Results

Demographics and Cognitive Assessment

The results of demographics and cognitive assessment are summarized in Table 1. There was no significant difference in age between groups ($P = 0.89$). The GLM on the cognitive scores revealed significant group effects ($P < 0.05$, see Table 1) on the IQ scores and number/numerosity comparison tasks. A significant group effect trend was observed for the simple subtraction task ($P = 0.06$).

Regarding the post hoc comparisons, the nonmosaic TS subjects had significantly lower IQ score values than the healthy controls (HC), with the exception of the VCI (Bonferroni corrected $P = 0.06$). The mosaic TS subjects scored lower than the HC on the FSIQ (Bonferroni corrected $P = 0.009$), PRI (Bonferroni corrected $P = 0.003$) and PSI (Bonferroni corrected $P = 0.002$). The 2 TS groups did not differ significantly regarding the 5 IQ scores. For the 2 math-related tasks showing a significant group effect, the nonmosaic TS subjects performed significantly worse than the HC in both the number comparison (Bonferroni corrected $P = 0.002$) and numerosity comparison (Bonferroni corrected $P = 0.009$). The mosaic TS subjects scored lower than the HC only in the numerosity comparison (Bonferroni corrected $P = 0.03$). The mosaic TS subjects outperformed the nonmosaic TS subjects only in the number comparison (Bonferroni corrected $P = 0.02$).

The X Chromosome Effects on GM Morphology

The whole-brain volume did not differ between groups ($P = 0.45$). The repeated-measures GLM revealed a significant main group effect on cortical thickness ($P = 0.01$). The post hoc comparisons indicated a significant difference only between the HC and nonmosaic TS subjects (Bonferroni corrected $P = 0.01$). A significant "region × group" interaction on cortical thickness was observed ($P < 0.001$), suggesting a spatially localized effect. Furthermore, the GLM analysis at the regional level (78 AAL regions in total) revealed significant group effects on thickness in 8 cortical regions (FDR corrected $P < 0.05$, see Supplementary Table 1), including the left/right inferior temporal gyrus, left/right middle temporal gyrus, right lingual gyrus, right superior temporal gyrus, right posterior cingulate gyrus, and right precuneus, as illustrated in Figure 2*A*. The post hoc comparisons found that nonmosaic TS had a greater thickness in each of the 8 regions than HC (Bonferroni corrected $P < 0.05$) but showed no significant difference with mosaic TS. Additionally, mosaic TS had a greater thickness than HC in these regions, with the exception of the right precuneus (Bonferroni corrected $P = 0.52$) and right middle temporal gyrus (Bonferroni corrected $P = 0.12$).

Regarding the cortical surface area, the repeated-measures GLM also showed a significant group effect ($P < 0.001$), and the post hoc comparisons indicated that the HC had significantly larger surface area than both mosaic (Bonferroni corrected $P < 0.001$) and nonmosaic TS subjects (Bonferroni corrected $P < 0.001$); the 2 TS groups did not differ significantly (Bonferroni corrected $P = 0.09$). As well, there was a significant "region × group" interaction ($P < 0.001$). The regional

Table 1
Demographics and cognitive testing

	Healthy control (n = 21)	Mosaic TS (n = 13)	Nonmosaic TS (n = 21)	Group effect (P-value)	Post hoc pairwise comparison (Bonferroni-corrected P-value)		
					HC/mTS	HC/nTS	mTS/nTS
Age (years)	14.0 ± 2.2	14.4 ± 2.2	14.2 ± 2.8	0.89	—	—	—
GH use	—	10	19	—	—	—	—
ER use	—	2	4	—	—	—	—
IQ scales							
FSIQ	109.2 ± 15.3 (20)	89.6 ± 17.0 (10)	89.1 ± 16.3 (16)	0.0005	0.009	0.002	1.00
WMI	101.7 ± 15.7 (20)	92.7 ± 14.6 (10)	88.3 ± 16.1 (16)	0.04	0.42	0.03	1.00
VCI	117.2 ± 14.2 (20)	102.6 ± 19.5 (10)	103.0 ± 20.6 (16)	0.03	0.12	0.06	1.00
PRI	103.4 ± 13.4 (20)	84.1 ± 17.3 (10)	84.3 ± 14.1 (16)	0.0003	0.003	0.0009	1.00
PSI	103.8 ± 16.1 (20)	83.9 ± 10.5 (10)	84.5 ± 11.8 (16)	0.0001	0.002	0.0003	1.00
Math tasks							
Number comparison	56.9 ± 11.8 (20)	55.5 ± 9.4 (13)	42.2 ± 17.2 (20)	0.001	1.00	0.002	0.02
Numerosity comparison	26.6 ± 6.0 (20)	21.4 ± 7.0 (13)	20.5 ± 6.6 (20)	0.006	0.03	0.009	1.00
Simple subtraction	44.2 ± 7.6 (20)	39.2 ± 10.1 (13)	37.0 ± 11.4 (20)	0.06	—	—	—

The parentheses after the cognitive scores represent the number of subjects who successfully performed the cognitive test. The Bonferroni correction was further applied for the post hoc pairwise comparisons if an overall group effect was found to be significant. GH, growth hormone; ER, estrogen replacement; HC, healthy control; mTS, mosaic Turner syndrome; nTS, nonmosaic Turner syndrome; FSIQ, full scale intelligence quotient; WMI, working-memory index; VCI, verbal comprehension index; PRI, perceptual reasoning index; PSI, processing speed index.

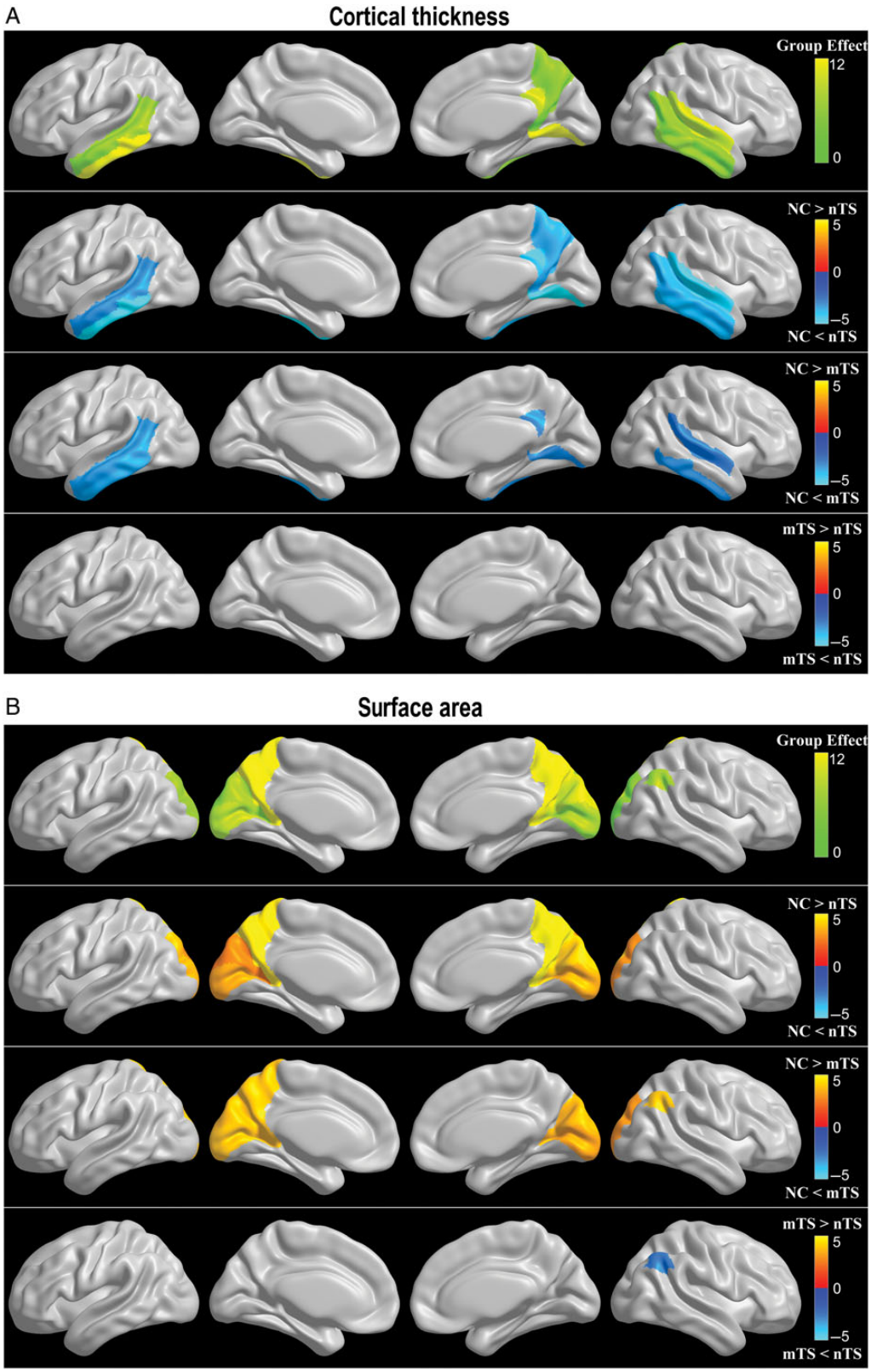

Figure 2. Cortical regions showing significant group differences in cortical thickness or surface area. (*A*) Cortical thickness; (*B*) Surface area. For both *A* and *B*, the first row represents the main group effect, and the next 3 rows indicate the post hoc comparison of HC versus nTS, HC versus mTS, and mTS versus nTS, respectively. In the first row, the color represents the *F* statistic for the main group effect. In the other rows, the color indicates the *T* statistic for the pair-wise comparison. HC, healthy control; nTS, nonmosaic Turner syndrome; mTS, mosaic Turner syndrome.

GLM analyses revealed significant group effects in 9 regions (FDR corrected $P < 0.05$): left/right precuneus, left/right cuneus, left/right calcarine fissures and surrounding cortex, left/right superior occipital gyrus, and right angular gyrus (Fig. 2*B* and Supplementary Table 2). With the exception of the left superior occipital gyrus, right precuneus, and right angular gyrus, the HC had a larger surface area than both TS groups in the remaining 6 cortical regions (Bonferroni corrected $P < 0.05$); no significant differences in these regions were found between the 2 TS groups. For the left superior occipital gyrus and right precuneus, the HC had a significantly larger surface area than the nonmosaic TS (Bonferroni corrected $P < 0.05$) subjects, and the mosaic TS subjects did not differ from either the HC or nonmosaic TS groups in this regard. In contrast, for the right angular gyrus, there was no significant difference between the HC and nonmosaic TS subjects, both of which showed a larger surface area than the mosaic TS subjects (Bonferroni corrected $P < 0.05$).

The repeated-measures GLM revealed a significant main group effect on the sub-cortical volume ($P = 0.02$), and the post hoc comparisons found a significant difference only between the HC and nonmosaic TS groups (Bonferroni corrected $P = 0.02$). However, no significant "region × group" interaction was observed here ($P = 0.11$), suggesting a diffuse effect of the X chromosome loss on the sub-cortical volume. Therefore, we did not perform further regional GLM analysis on each sub-cortical structure, separately.

The X Chromosome Effects on WM Connectivity

First, the repeated-measures GLM revealed a significant main group effect on both FA ($P < 0.001$) and MD ($P < 0.001$). The post hoc comparisons found that the HC had a significantly higher FA and lower MD than both mosaic (FA: Bonferroni corrected $P = 0.002$; MD: Bonferroni corrected $P = 0.02$) and nonmosaic TS subjects (FA: Bonferroni corrected $P < 0.001$; MD: Bonferroni corrected $P < 0.001$), but the 2 TS groups did not differ. A significant "region × group" interaction was found for FA ($P < 0.001$) but not for MD ($P = 0.76$). This implied that the effect of X chromosome loss was spatially localized for FA, but was spatially diffuse for MD. Consequently, separate GLM analysis was applied to each WMPM region (68 in total) only for FA, and the results are summarized in Supplementary Tables 3. Specifically, FA showed a significant group effect in 45 WMPM regions (FDR corrected $P < 0.05$), as illustrated in Figure 3. Notably, among the WMPM regions showing significant group effects, the strongest effect primarily involved the WM tracts/regions connecting or adjacent to the temporal, occipital, and parietal cortices. The top 5 regions with the greatest effect on FA were the left/right temporal blade, left/right occipital blade, and right superior parietal blade (Table 2).

Among the 53 WMPM regions showing significant group effects on FA (FDR corrected $P < 0.05$), the post hoc comparisons indicated that the nonmosaic TS group had a lower FA than the HC in 50 regions but showed a lower FA than the mosaic TS subjects in only the left tapetum (Fig. 3*A*). Additionally, the mosaic

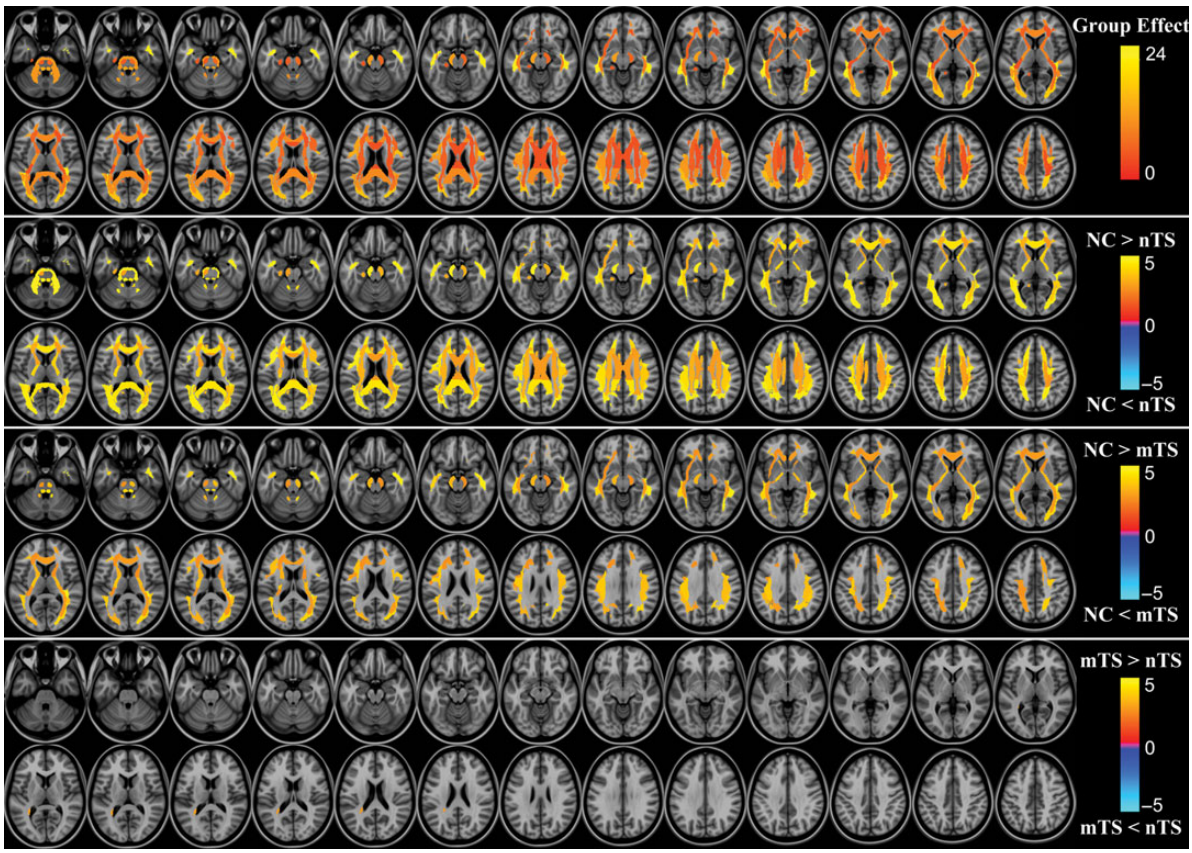

Figure 3. WMPM regions showing significant group differences in FA. The first row represents the main group effect, and the next 3 rows indicate the post hoc comparison of HC versus nTS, HC versus mTS, and mTS versus nTS, respectively. In the first row, the color represents the *F* statistic for the main group effect. In the other rows, the color indicates the *T* statistic for the pair-wise comparison. HC, healthy control; nTS, nonmosaic Turner syndrome; mTS, mosaic Turner syndrome.

Table 2
The top 5 WMPM regions showing the strongest group effects for FA

WMPM regions	Healthy control ($n = 21$)	Mosaic TS ($n = 13$)	Nonmosaic TS ($n = 21$)	Group effect (q-value $\times 10^{-4}$)	Post hoc pairwise comparisons (Bonferroni-corrected P-value)		
					HC/mTS	HC/nTS	mTS/nTS
Temporal blade (R)	0.43 ± 0.02	0.40 ± 0.02	0.40 ± 0.01	0.02	0.00	0.00	1.00
Temporal blade (L)	0.44 ± 0.02	0.42 ± 0.02	0.41 ± 0.02	0.03	0.00	0.00	0.21
Superior parietal blade (R)	0.42 ± 0.02	0.39 ± 0.02	0.39 ± 0.02	0.32	0.00	0.00	0.84
Occipital blade (R)	0.39 ± 0.02	0.37 ± 0.02	0.37 ± 0.02	0.37	0.00	0.00	1.00
Occipital blade (L)	0.40 ± 0.02	0.39 ± 0.02	0.38 ± 0.02	0.53	0.01	0.00	0.33

The q-values represent the corrected P-values after the FDR correction for multiple comparisons across different regions when testing the group effects (Genovese et al. 2002). The Bonferroni correction was further applied for the post hoc pairwise comparisons if an overall group effect was found to be significant. WMPM, white matter parcellation map (Mori et al. 2008); HC, healthy control; mTS, mosaic Turner syndrome; nTS, nonmosaic Turner syndrome; (L), left side; (R), right side.

TS subjects had a significantly lower FA than the HC in 35 of the 53 WMPM regions.

As a validation analysis, we additionally tested the main group effects on the cortical thickness/surface area at the vertex level and the FA/MD at the voxel level. As illustrated in Supplementary Figure 1, the results at the vertex/voxel level were highly convergent with the current findings at the regional level (Figs 2 and 3).

X Chromosome Effects on the Brain–cognition Relationship

To determine the effect of X chromosome loss on the brain–cognition relationship, the "brain measure × group" interaction was tested for each of the cognitive items. A significant interaction here indicated a significant difference in regression slopes for the brain measures (e.g., cortical thickness, surface area, sub-cortical volume, FA, and MD) between groups. As listed in Table 3, there were significant "brain × group" interactions (FDR corrected $P < 0.05$) for 3 IQ scores (i.e., FSIQ, PRI, and WMI) but not for any of the math task scores. Specifically, we found a significant "thickness × group" interaction on FSIQ in 3 cortical regions (right middle frontal gyrus, right superior dorsolateral frontal gyrus, and left rolandic operculum) on PRI in the right middle frontal gyrus and on WMI in 16 cortical regions (Table 3). Additionally, a significant "area × group" interaction on FSIQ was also observed in the left middle temporal pole. No sub-cortical structures showed a significant "volume × group" interaction on any of the cognitive scores, and no WMPM regions had a significant "FA × group" or MD × group" interaction. As illustrated in Figure 4 and Supplementary Figure 2, for the cortical regions with a significant "thickness/area × group" interaction, IQ scores correlated positively with thickness/area in the HC group but negatively in the 2 TS groups. The patterns of the brain–cognition relationship were largely similar among the 2 TS groups.

Finally, to evaluate the effects of covarying the age and the whole-brain volume, we reran all analyses after excluding them from our statistical model when applicable. The results are highly consistent with our current findings (data not shown).

Discussion

Using a cohort of adolescent mosaic and nonmosaic TS patients and controls, the present study performed a comprehensive investigation to reveal the role of the X chromosome in brain morphology and connectivity and their relationships with cognition. Intriguingly, the comparative analyses found significant "X chromosome dosage effects", that is, differences between the mosaic and nonmosaic TS groups in the cortical surface area in the right angular gyrus, as well as in WM integrity of the left tapetum of corpus callosum. Furthermore, the results demonstrated that the X chromosome plays a significant role in modulating the relationship between cortical morphology and the WMI in multiple cortical regions such as the right middle frontal gyrus and the right superior dorsolateral frontal gyrus. These findings provide novel information for the role of the X chromosome on human neuroanatomy and cognition during development, which has great implication for understanding the sex difference in brain and cognition.

Neuroanatomical Differences Between TS Patients and Healthy Controls During Adolescence

For genetic disorders such as TS, it is important to separately analyze the 2 lower-order components of cortical volume, cortical thickness, and surface area, because the 2 components have shown independent genetic determinants (Panizzon et al. 2009). In the present study, the observed increases in cortical thickness but decreases in surface area for the TS patients are highly convergent with previous findings (Raznahan et al. 2010; Lepage, Mazaika, et al. 2013; Lepage, Hong, et al. 2013). Specifically, the increased cortical thickness in the TS subjects was primarily located around the bilateral dorsolateral temporal lobes, which is likely to be the reason for the enlargement of temporal lobe cortical volume (Kesler et al. 2003; Rae et al. 2004). In contrast, the decreases in surface area primarily affected the parieto-occipital lobes; this was likely a main driving factor for the parieto-occipital GM reduction in the TS subjects (Reiss et al. 1995; Brown et al. 2002; Molko et al. 2004; Marzelli et al. 2011). Notably, the cortical spatial pattern of the TS-associated changes were quite different between the thickness and surface area, which further emphasizes different genetic basis for the 2 cortical measures and favors separate analysis on cortical thickness and surface area for genetic analysis on cortical morphology.

In addition to the GM morphology, 2 DTI studies reported FA or MD changes in specific WM tracts (such as the superior longitudinal fasciculus in TS patients) compared with healthy controls (Holzapfel et al. 2006; Yamagata et al. 2012). The present study observed a more diffusive pattern of disrupted WM integrity (i.e., decreased FA and increased MD) in both of the TS groups. Notably, despite the diffusive change pattern, the strongest X chromosome effect primarily involved the tracts/regions connecting or adjacent to the temporal, occipital,

Table 3
The significant "brain measure × group" interactions for the cognitive scores

Cognition	Cortical regions	Thickness × group		Area × group	
		F	*q*-value	*F*	*q*-value
FSIQ	Middle temporal pole (L)	NS	NS	9.38	0.038
	Middle frontal gyrus (R)	11.93	0.008	NS	NS
	Superior dorsolateral frontal gyrus (R)	8.22	0.042	NS	NS
	Rolandic operculum (L)	7.58	0.044	NS	NS
PRI	Middle frontal gyrus (R)	9.62	0.032	NS	NS
WMI	Middle frontal gyrus (R)	12.36	0.006	NS	NS
	Precentral gyrus (L)	10.48	0.008	NS	NS
	Superior dorsolateral frontal gyrus (R)	10.01	0.008	NS	NS
	Rolandic operculum (L)	8.79	0.014	NS	NS
	Precuneus (R)	7.70	0.021	NS	NS
	Inferior parietal gyrus (L)	7.63	0.021	NS	NS
	Angular gyrus (L)	7.27	0.024	NS	NS
	Inferior occipital gyrus (L)	6.78	0.027	NS	NS
	Superior dorsolateral frontal gyrus (L)	6.69	0.027	NS	NS
	Superior temporal gyrus (L)	6.61	0.027	NS	NS
	Median cingulate gyri (L)	6.39	0.028	NS	NS
	Precentral gyrus (R)	6.31	0.028	NS	NS
	Supramarginal gyrus (L)	5.90	0.035	NS	NS
	Supramarginal gyrus (R)	5.34	0.048	NS	NS
	Cuneus (L)	5.27	0.048	NS	NS
	Orbital superior frontal gyrus (R)	5.23	0.048	NS	NS

The *q*-values represent the corrected *P*-values after the FDR correction for multiple comparisons across different regions when testing the "brain measure × group" effects (Genovese et al. 2002). FSIQ, full scale intelligence quotient; WMI, working-memory index; PRI, perceptual reasoning index; (L), left side; (R), right side; NS, not significant.

and parietal cortices. Together with cortical morphology findings, it appears that the loss of the X chromosome primarily influences the parietal-temporal-occipital neural system. However, it remains to be determined whether the abnormalities in GM and WM observed here are caused independently or have a causal relationship. Putatively, structural anomalies in both GM and WM should jointly underlie the abnormalities in functional activity and connectivity in TS patients (Molko et al. 2003; Hart et al. 2006; Bray et al. 2011, 2013).

"X chromosome Dosage Effects" on Neuroanatomical Phenotypes During Adolescence

The present study was the first to include mosaic TS patients as an independent group when studying cortical morphology and WM connectivity; this method enabled the testing of the "X chromosome dosage effect" on these brain measures. As proposed previously (Murphy et al. 1993, 1997), a significant difference between mosaic and nonmosaic TS indicates an "X chromosome dosage effect", which suggests a phenotypic dependence on the X chromosome dosage. The lack of such a dosage effect implies a binary/categorical consequence of X chromosome loss, reflecting nonspecific anatomical responses to genomic effects of altered X chromosome dosage.

Among the GM measures, only the surface area of the right angular gyrus exhibited a significant difference between the 2 TS groups, with a similar trend observed in the left superior occipital gyrus (uncorrected $P < 0.05$). Accumulating evidence has demonstrated that the angular gyrus supports very complex brain functions and is involved in multiple high-level cognitive processes such as language, math, and memory (Seghier 2013). Both structural and functional alterations in the angular gyrus have been repeatedly found in TS (Haberecht et al. 2001; Molko et al. 2003; Kesler et al. 2006), suggesting a link between this structure and the X chromosome. The observed "X chromosome dosage effect" here sheds further light on the relationship between the X chromosome and this structure. Intriguingly, the direction of the group differences was unexpected to some degree: the surface area of the right angular gyrus in the mosaic TS subjects was smaller than those of both the control and nonmosaic TS subjects. This finding suggests that neuroanatomical changes do not necessarily follow a monotonic pattern as the X chromosome loss increases. In contrast, the surface area of the left superior occipital gyrus in the mosaic TS subjects was intermediate between that of the control and nonmosaic TS; this finding was compatible with a linear function of the X chromosome dosage and brain structure in this scenario. Given its significant role in visuo-spatial processing (Kesler et al. 2004), the smaller area of the left superior occipital gyrus may relate to the less severe visuo-spatial impairment in mosaic TS compared with nonmosaic TS (Rovet 2004).

Among the WM measures, only the FA of the left tapetum of corpus callosum exhibited an "X chromosome dosage effect": the nonmosaic TS group showed a deceased FA compared with the mosaic TS group. This suggests a positive effect of the X chromosome dosage on WM integrity. Given the X dosage effect on the corpus callosum, an inferior interhemispheric communication was expected in nonmosaic TS, which may be associated with worse performance in most cognitive tasks compared with mosaic TS (Rovet 2004).

Finally, it should be noted that Murphy et al. (1993) reported "X chromosome dosage effects" on the lenticular and thalamic nuclei volume, which the present study failed to detect. These discrepant results may be due to the differences in the age range of samples (adults vs. adolescents), neuroimaging acquisition techniques or methods of analysis.

The X Chromosome's Role in the Brain–cognition Relationship During Adolescence

Intriguingly, the current study observed significant changes in the relationship between cortical morphology and IQ scores in specific cortical regions, as indicated by significant "cortical thickness/surface area × group" interactions for the IQ scores. These results suggest that some genes on the X chromosome

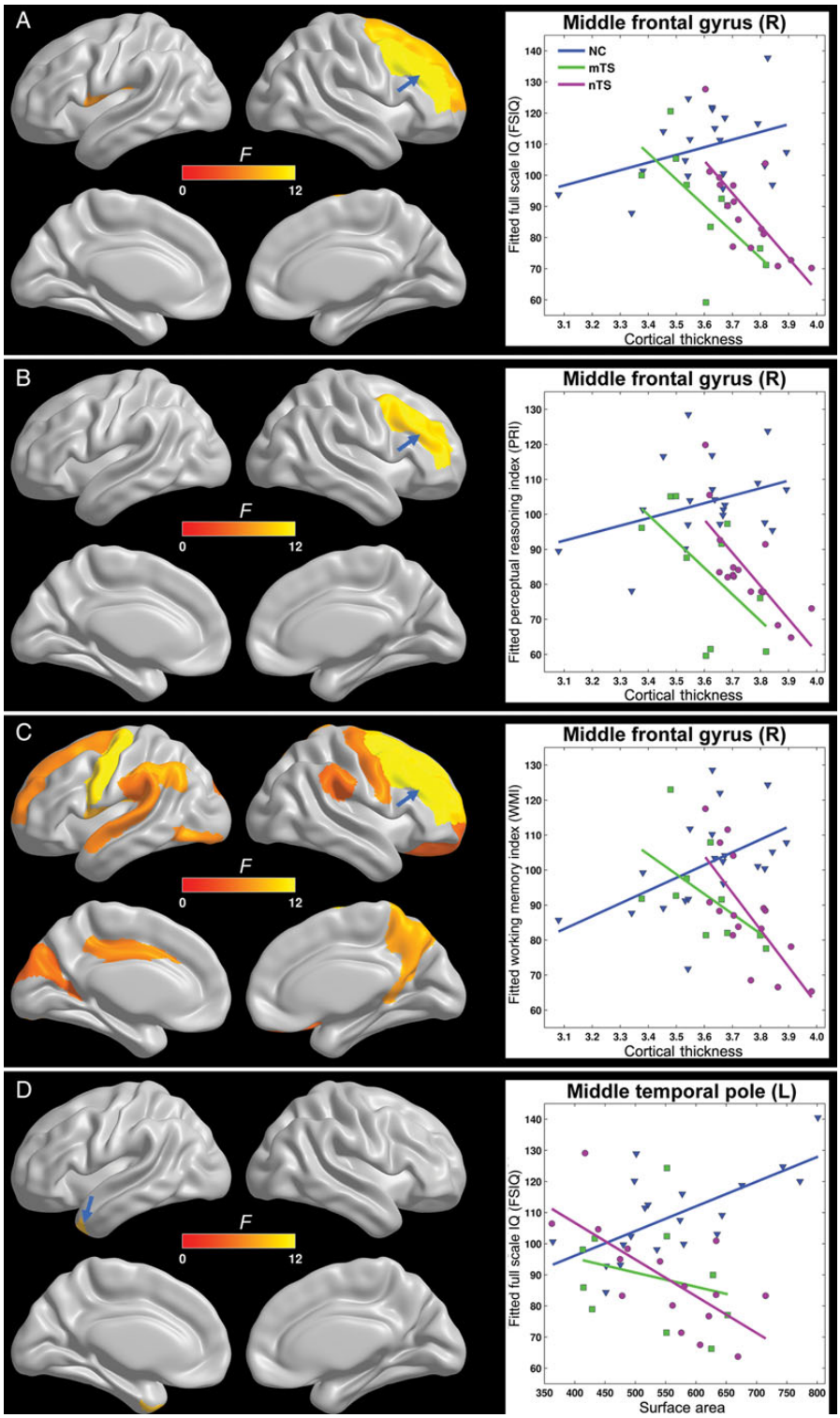

Figure 4. Cortical regions showing significant brain × group interactions on the cognitive scores. (*A*) The regions showing cortical thickness × group interactions with regard to FSIQ. (*B*) The regions showing cortical thickness × group interactions with regard to the PRI. (*C*) The regions showing cortical thickness × group interactions with regard to the WMI. (*D*) The regions showing surface area × group interactions with regard to FSIQ. The color on the cortical regions represents the *F* value for the corresponding interaction. Due to limited space, the scatter plot was provided only for the region with the most significant interaction. The selected region is indicated by the blue arrow on the surface. The scatter plots for all significant regions are present in Supplementary Figure 2. FSIQ, full scale IQ; PRI, perceptual reasoning index; WMI, working-memory index.

may act as modulators in the brain–cognition relationship. Note that the alteration of the brain–cognition relationship does not necessarily mean a significant group change in brain measures and vice versa. This finding is of particular implication for cognitive studies, in which the same brain–cognition relation is typically presumed across both healthy and patient populations.

Specifically, the majority of detected differences in the brain–cognition relationship between TS and controls are between cortical thickness and the WMI of the IQ test. The alterations of the thickness–WMI relationship were primarily located in the association cortex (locations such as the right middle frontal gyrus, right superior dorsolateral frontal gyrus, and left inferior parietal gyri, most of which have been previously reported as related to working memory) (Baddeley 2003). We also observed changes in the thickness–FSIQ relationship in the right middle frontal gyrus, right superior dorsolateral frontal gyrus, and left rolandic operculum, which are likely attributable to the detected changes in the thickness–WMI relationship in these regions (given the substantial contribution of WMI to the FSIQ score).

In healthy girls, both the cortical thickness and surface area showed a positive correlation with IQ; this finding was compatible with previous IQ studies (Shaw et al. 2006). However, these relationships were consistently reversed in both the mosaic and nonmosaic TS patients: the IQ scores increases with reductions in thickness. This negative correlation in TS patients is compatible with the group differences between TS patients and controls (where TS patients had an increased thickness but a decreased IQ score). The direction of the brain–cognition relationship did not differ between the mosaic and nonmosaic TS subjects, though the slopes differed in a couple of regions, such as the left middle cingulate gyrus. The dramatic alterations in the brain–cognition relationship due to X chromosome loss highlight the necessity of taking the brain–gene interactions into account when predicting human cognition abilities (Schmidt et al. 2009). Particularly, more attention should be paid to the role of genetic factors on the brain–cognition relationship in the context of understanding cognitive profiles of brain diseases (especially the genetic ones).

Direct Genetic Effect or Indirect Hormonal Effect

X-linked genes are known to affect the brain at least in 2 ways: by directly acting on the brain and by indirectly acting on the gonads to induce differences in specific gonadal secretions (i.e., hormones) that have specific effects on the brain (Arnold 2004). To isolate the direct genetic effect from the indirect hormonal effect, one possible approach is to ensure identical hormonal levels across individuals with different X-linked genotypes. However, hormonal deficits due to gonadal dysgenesis are extremely common in TS; therefore, in our case, it is difficult to differentiate between the direct genetic effect of the X chromosome and the indirect hormonal effect on the brain. Our observed neuroanatomical and cognitive phenotypes in TS patients could be due to a direct genetic factor, an indirect hormonal factor, or a combination of the 2.

Although identical hormone levels between adolescent TS patients and healthy controls are difficult to achieve in practice, a suboptimal alternative is to match the pubertal stage, as an approximate for the sex hormone level, between groups. Unfortunately, despite of the age range from 9 to 18 years, the majority of TS patients in the present study were at the prepubertal stage (i.e., pubertal stage I) because spontaneous puberty development is very rare in TS girls (Pasquino et al. 1997; Bannink et al. 2009), and most of our TS patients did not undergo ER to artificially induce puberty development.

Nonetheless, we reanalyzed the data with only subjects at the prepubertal stage (age: 9–12 years), including 8 controls, 8 nonmosaic, and 3 mosaic TS patients. This additional analysis approximately ensured the matching in both age and pubertal status between the TS patients and controls. Intriguingly, the spatial patterns of statistical results for the pre-pubertal stage (data not shown) are largely similar with those from the entire cohort, favoring a direct genetic effect for our current findings. A larger cohort matching for both age and pubertal status between TS patients and controls is desired to confirm our findings in the future.

While animal models are essential to dissociate the genetic and hormonal effects (Arnold and Chen 2009; Raznahan et al. 2013), other human MRI studies have also provided important clues on this issue. For example, cortical thinning of the temporal cortex has been found in 47XXY men compared with 46XX women and 46XY men (Savic and Arver 2014). This finding is reciprocal to the comparatively thickening temporal cortex found in 45XO girls. Given that the sex steroids are low in both 47XXY males and 45XO females, a direct genetic effect on the thickness of the temporal cortex is more likely. Moreover, the observed neuroanatomical differences between the nonmosaic and mosaic TS patients (i.e., "X chromosome dosage effect") imply a direct genetic effect: both TS had gonadal dysgenesis but had different amounts of the X chromosome (Murphy et al. 1997).

However, a few studies have also demonstrated significant correlations between hormone levels and neuroanatomical phenotypes such as the GM volume of the amygdala and parahippocampus (Lentini et al. 2013). Particularly, in summarizing MRI findings of the human brain, a recent review found consistent changes of the medial temporal lobe structures among different endocrine disorders with either sex steroid excess or deficiency (Mueller 2013), therefore supporting an indirect hormonal effect on related brain structures rather than a direct genetic effect.

Limitations

Finally, a few caveats need to be addressed. First, despite the scarceness of TS patients and a narrow age range limit, we collected a relatively large number of samples compared with other TS studies. However, the absolute sample size remains small. Additionally, the mosaic TS group had fewer samples than the other 2 groups, resulting in a difference in the statistical power between post hoc pairwise comparisons. Further, mosaic TS patients with similar proportions of cells missing the entire second X chromosome are difficult to match, given the limited number of volunteers available. Therefore, our current mosaic group was heterogeneous in terms of the cell proportion. Furthermore, while the mosaicism was confirmed using a peripheral blood sample, it remains unknown if a detected mosaicism in the blood can indicate a mosaicism in brain. Third, factors such as GH use, ER treatment, and X-linked imprinting may also influence the brain structures in TS (Kesler et al. 2003; Cutter et al. 2006; Lepage, Clouchoux, et al. 2013; Lepage, Hong, et al. 2013; Lepage, Hong, et al. 2012). Due to the limited sample size and the lack of related information, it is not feasible to evaluate their effects in the present study. Future studies with a large sample size are warranted to test these potential confounding factors. Lastly, by design, the present study focused on a limited age range of adolescence, which provides a valuable opportunity for understanding the X chromosome effects on the brain and cognitive

development. Caution should be exercised when extrapolating these findings across the entire life span.

Conclusion

By showing differences between mosaic and nonmosaic TS patients, the present study revealed "X chromosome dosage effects" on cortical surface area and WM connectivity, supporting a link between the brain structural phenotypes and the type of X chromosome loss. Furthermore, the relationship between the cortical morphology and WMI exhibited dramatic alterations in both TS patient types in specific regions, suggesting that the X chromosome modulates specific brain–cognition relationships. These novel findings provide new insights into how the X chromosome affects the human brain, and suggest an important role of genetic factors in brain–cognition relationships.

Supplementary Material

Supplementary material can be found at: http://www.cercor.oxfordjournals.org/.

Funding

This work was supported by the 973 program (no. 2013CB837300), the National Science Foundation of China (nos 81271649, 81322021, 31000499, 31222024 and 31221003), the Beijing Nova Program (no. Z121110002512032), the Specialized Research Fund for the Doctoral Program of Higher Education, China (no. 20130003110002), the Major Project of National Social Science Foundation (no. 12&ZD228), the Scientific Research Foundation for the Returned Overseas Chinese Scholars, and the Open Research Fund of the National Key Laboratory of Cognitive Neuroscience and Learning, China.

Notes

The authors thank Prof. Alan Evans for providing the CIVET tool during the cortical morphological analysis. The authors thank Prof. Xinlin Zhou for the helps during the math-related cognitive testing. Also, the authors sincerely thank the 3 anonymous reviewers for their thoughtful and constructive comments. *Conflict of Interest*: None declared.

References

Arnold AP. 2004. Sex chromosomes and brain gender. Nat Rev Neurosci. 5:701–708.

Arnold AP, Chen X. 2009. What does the "four core genotypes" mouse model tell us about sex differences in the brain and other tissues? Front Neuroendocrinol. 30:1–9.

Baddeley A. 2003. Working memory: looking back and looking forward. Nat Rev Neurosci. 4:829–839.

Bannink EM, van Sassen C, van Buuren S, de Jong FH, Lequin M, Mulder PG, de Muinck Keizer-Schrama SM. 2009. Puberty induction in Turner syndrome: results of oestrogen treatment on development of secondary sexual characteristics, uterine dimensions and serum hormone levels. Clin Endocrinol. 70:265–273.

Beaulieu C. 2002. The basis of anisotropic water diffusion in the nervous system—a technical review. NMR Biomed. 15:435–455.

Bray S, Dunkin B, Hong DS, Reiss AL. 2011. Reduced functional connectivity during working memory in Turner syndrome. Cereb Cortex. 21:2471–2481.

Bray S, Hoeft F, Hong DS, Reiss AL. 2013. Aberrant functional network recruitment of posterior parietal cortex in turner syndrome. Hum Brain Mapp. 34:3117–3128.

Brown WE, Kesler SR, Eliez S, Warsofsky IS, Haberecht M, Patwardhan A, Ross JL, Neely EK, Zeng SM, Yankowitz J et al. 2002. Brain development in Turner syndrome: a magnetic resonance imaging study. Psychiatry Res Neuroimage 116:187–196.

Carrel L, Cottle AA, Goglin KC, Willard HF. 1999. A first-generation X-inactivation profile of the human X chromosome. Proc Natl Acad Sci USA. 96:14440–14444.

Cui Z, Zhong S, Xu P, He Y, Gong G. 2013. PANDA: a pipeline toolbox for analyzing brain diffusion images. Front Hum Neurosci. 7:42.

Cutter WJ, Daly EM, Robertson DM, Chitnis XA, van Amelsvoort TA, Simmons A, Ng VW, Williams BS, Shaw P, Conway GS et al. 2006. Influence of X chromosome and hormones on human brain development: a magnetic resonance imaging and proton magnetic resonance spectroscopy study of Turner syndrome. Biol Psychiatry. 59:273–283.

Disteche CM. 1999. Escapees on the X chromosome. Proc Natl Acad Sci USA. 96:14180–14182.

Engqvist L. 2005. The mistreatment of covariate interaction terms in linear model analyses of behavioural and evolutionary ecology studies. Anim Behav. 70:967–971.

Genovese CR, Lazar NA, Nichols T. 2002. Thresholding of statistical maps in functional neuroimaging using the false discovery rate. Neuroimage. 15:870–878.

Gong G, He Y, Chen ZJ, Evans AC. 2012. Convergence and divergence of thickness correlations with diffusion connections across the human cerebral cortex. Neuroimage. 59:1239–1248.

Gravholt CH. 2005. Clinical practice in Turner syndrome. Nat Clin Pract Endocrinol Metab. 1:41–52.

Haberecht MF, Menon V, Warsofsky IS, White CD, Dyer-Friedman J, Glover GH, Neely EK, Reiss AL. 2001. Functional neuroanatomy of visuo-spatial working memory in Turner syndrome. Hum Brain Mapp. 14:96–107.

Hart SJ, Davenport ML, Hooper SR, Belger A. 2006. Visuospatial executive function in Turner syndrome: functional MRI and neurocognitive findings. Brain. 129:1125–1136.

Holzapfel M, Barnea-Goraly N, Eckert MA, Kesler SR, Reiss AL. 2006. Selective alterations of white matter associated with visuospatial and sensorimotor dysfunction in Turner syndrome. J Neurosci. 26:7007–7013.

Hong DS, Reiss AL. 2012. Cognition and behavior in Turner syndrome: a brief review. Pediatr Endocrinol Rev. 9(Suppl 2):710–712.

Jenkinson M, Beckmann CF, Behrens TE, Woolrich MW, Smith SM. 2012. FSL. Neuroimage. 62:782–790.

Johnson W, Carothers A, Deary IJ. 2009. A role for the XChromosome in sex differences in variability in general intelligence? Perspect Psychol Sci. 4:598–611.

Kesler SR, Blasey CM, Brown WE, Yankowitz J, Zeng SM, Bender BG, Reiss AL. 2003. Effects of X-monosomy and X-linked imprinting on superior temporal gyrus morphology in Turner syndrome. Biol Psychiatry. 54:636–646.

Kesler SR, Haberecht MF, Menon V, Warsofsky IS, Dyer-Friedman J, Neely EK, Reiss AL. 2004. Functional neuroanatomy of spatial orientation processing in Turner syndrome. Cereb Cortex. 14:174–180.

Kesler SR, Menon V, Reiss AL. 2006. Neurofunctional differences associated with arithmetic processing in turner syndrome. Cereb Cortex. 16:849–856.

Kim JS, Singh V, Lee JK, Lerch J, Ad-Dab'bagh Y, MacDonald D, Lee JM, Kim SI, Evans AC. 2005. Automated 3-D extraction and evaluation of the inner and outer cortical surfaces using a Laplacian map and partial volume effect classification. Neuroimage. 27:210–221.

Laumonnier F, Cuthbert PC, Grant SG. 2007. The role of neuronal complexes in human X-linked brain diseases. Am J Hum Genet. 80:205–220.

Lehrke R. 1972. Theory of X-linkage of major intellectual traits. Am J Ment Defic. 76:611–619.

Lentini E, Kasahara M, Arver S, Savic I. 2013. Sex differences in the human brain and the impact of sex chromosomes and sex hormones. Cereb Cortex. 23:2322–2336.

Lepage JF, Clouchoux C, Lassonde M, Evans AC, Deal CL, Theoret H. 2013. Abnormal motor cortex excitability is associated with reduced cortical thickness in X monosomy. Hum Brain Mapp. 34:936–944.

Lepage JF, Hong DS, Hallmayer J, Reiss AL. 2012. Genomic imprinting effects on cognitive and social abilities in prepubertal girls with Turner syndrome. J Clin Endocrinol Metab. 97:E460–E464.
Lepage JF, Hong DS, Mazaika PK, Raman M, Sheau K, Marzelli MJ, Hallmayer J, Reiss AL. 2013. Genomic imprinting effects of the X chromosome on brain morphology. J Neurosci. 33:8567–8574.
Lepage JF, Mazaika PK, Hong DS, Raman M, Reiss AL. 2013. Cortical brain morphology in young, estrogen-naive, and adolescent, estrogen-treated girls with Turner syndrome. Cereb Cortex. 23:2159–2168.
Lerch JP, Evans AC. 2005. Cortical thickness analysis examined through power analysis and a population simulation. Neuroimage. 24:163–173.
Lyttelton OC, Karama S, Ad-Dab'bagh Y, Zatorre RJ, Carbonell F, Worsley K, Evans AC. 2009. Positional and surface area asymmetry of the human cerebral cortex. Neuroimage. 46:895–903.
MacDonald D, Kabani N, Avis D, Evans AC. 2000. Automated 3-D extraction of inner and outer surfaces of cerebral cortex from MRI. Neuroimage. 12:340–356.
Marzelli MJ, Hoeft F, Hong DS, Reiss AL. 2011. Neuroanatomical spatial patterns in Turner syndrome. Neuroimage. 55:439–447.
Molko N, Cachia A, Riviere D, Mangin JF, Bruandet M, Le Bihan D, Cohen L, Dehaene S. 2003. Functional and structural alterations of the intraparietal sulcus in a developmental dyscalculia of genetic origin. Neuron. 40:847–858.
Molko N, Cachia A, Riviere D, Mangin JF, Bruandet M, LeBihan D, Cohen L, Dehaene S. 2004. Brain anatomy in Turner syndrome: evidence for impaired social and spatial-numerical networks. Cereb Cortex. 14:840–850.
Mori S, Oishi K, Jiang H, Jiang L, Li X, Akhter K, Hua K, Faria AV, Mahmood A, Woods R. 2008. Stereotaxic white matter atlas based on diffusion tensor imaging in an ICBM template. NeuroImage. 40:570–582.
Mueller SC. 2013. Magnetic resonance imaging in paediatric psychoneuroendocrinology: a new frontier for understanding the impact of hormones on emotion and cognition. J Neuroendocrinol. 25:762–770.
Murphy DG, Mentis MJ, Pietrini P, Grady C, Daly E, Haxby JV, De La Granja M, Allen G, Largay K, White BJ et al. 1997. A PET study of Turner's syndrome: effects of sex steroids and the X chromosome on brain. Biol Psychiatry. 41:285–298.
Murphy DGM, Decarli C, Daly E, Haxby JV, Allen G, White BJ, Mcintosh AR, Powell CM, Horwitz B, Rapoport SI et al. 1993. X-chromosome effects on female brain—a magnetic resonance imaging study of Turners Syndrome. Lancet. 342:1197–1200.
Nguyen DK, Disteche CM. 2006a. Dosage compensation of the active X chromosome in mammals. Nat Genet. 38:47–53.
Nguyen DK, Disteche CM. 2006b. High expression of the mammalian X chromosome in brain. Brain Res. 1126:46–49.
Oishi K, Zilles K, Amunts K, Faria A, Jiang H, Li X, Akhter K, Hua K, Woods R, Toga AW et al. 2008. Human brain white matter atlas: identification and assignment of common anatomical structures in superficial white matter. Neuroimage. 43:447–457.
Panizzon MS, Fennema-Notestine C, Eyler LT, Jernigan TL, Prom-Wormley E, Neale M, Jacobson K, Lyons MJ, Grant MD, Franz CE et al. 2009. Distinct genetic influences on cortical surface area and cortical thickness. Cereb Cortex. 19:2728–2735.
Pasquino AM, Passeri F, Pucarelli I, Segni M, Municchi G. 1997. Spontaneous pubertal development in Turner's syndrome. Italian Study Group for Turner's Syndrome. J Clin Endocrinol Metab. 82:1810–1813.
Patenaude B, Smith SM, Kennedy DN, Jenkinson M. 2011. A Bayesian model of shape and appearance for subcortical brain segmentation. Neuroimage. 56:907–922.
Rae C, Joy P, Harasty J, Kemp A, Kuan S, Christodoulou J, Cowell CT, Coltheart M. 2004. Enlarged temporal lobes in Turner syndrome: an X-chromosome effect? Cereb Cortex. 14:156–164.
Raznahan A, Cutter W, Lalonde F, Robertson D, Daly E, Conway GS, Skuse DH, Ross J, Lerch JP, Giedd JN et al. 2010. Cortical anatomy in human X monosomy. Neuroimage. 49:2915–2923.
Raznahan A, Probst F, Palmert MR, Giedd JN, Lerch JP. 2013. High resolution whole brain imaging of anatomical variation in XO, XX, and XY mice. Neuroimage. 83:962–968.
Reiss AL, Mazzocco MM, Greenlaw R, Freund LS, Ross JL. 1995. Neurodevelopmental effects of X monosomy: a volumetric imaging study. Ann Neurol. 38:731–738.
Ropers HH, Hamel BC. 2005. X-linked mental retardation. Nat Rev Genet. 6:46–57.
Rovet J. 2004. Turner syndrome: A review of genetic and hormonal influences on neuropsychological functioning. Child Neuropsychol. 10:262–279.
Savic I, Arver S. forthcoming 2014. Sex differences in cortical thickness and their possible genetic and sex hormonal underpinnings. Cereb Cortex.
Schmidt LA, Fox NA, Perez-Edgar K, Hamer DH. 2009. Linking gene, brain, and behavior: DRD4, frontal asymmetry, and temperament. Psychol Sci. 20:831–837.
Seghier ML. 2013. The angular gyrus: multiple functions and multiple subdivisions. Neuroscientist. 19:43–61.
Shaw P, Greenstein D, Lerch J, Clasen L, Lenroot R, Gogtay N, Evans A, Rapoport J, Giedd J. 2006. Intellectual ability and cortical development in children and adolescents. Nature. 440:676–679.
Skuse DH. 2005. X-linked genes and mental functioning. Hum Mol Genet. 14(Spec No 1):R27–R32.
Sled JG, Zijdenbos AP, Evans AC. 1998. A nonparametric method for automatic correction of intensity nonuniformity in MRI data. IEEE Trans Med Imaging. 17:87–97.
Swingland JT, Durrenberger PF, Reynolds R, Dexter DT, Pombo A, Deprez M, Roncaroli F, Turkheimer FE. 2012. Mean expression of the X-chromosome is associated with neuronal density. Front Neurosci. 6:161.
Sybert VP, McCauley E. 2004. Turner's syndrome. N Engl J Med. 351:1227–1238.
Tohka J, Zijdenbos A, Evans A. 2004. Fast and robust parameter estimation for statistical partial volume models in brain MRI. Neuroimage. 23:84–97.
Turner G. 1996. Intelligence and the X chromosome. Lancet. 347:1814–1815.
Tzourio-Mazoyer N, Landeau B, Papathanassiou D, Crivello F, Etard O, Delcroix N, Mazoyer B, Joliot M. 2002. Automated anatomical labeling of activations in SPM using a macroscopic anatomical parcellation of the MNI MRI single-subject brain. Neuroimage. 15:273–289.
Wei W, Lu H, Zhao H, Chen C, Dong Q, Zhou X. 2012. Gender differences in children's arithmetic performance are accounted for by gender differences in language abilities. Psychol Sci. 23:320–330.
Yamagata B, Barnea-Goraly N, Marzelli MJ, Park Y, Hong DS, Mimura M, Reiss AL. 2012. White matter aberrations in prepubertal estrogen-naive girls with monosomic Turner Syndrome. Cereb Cortex. 22:2761–2768.
Zijdenbos AP, Forghani R, Evans AC. 2002. Automatic "pipeline" analysis of 3-D MRI data for clinical trials: application to multiple sclerosis. IEEE Trans Med Imaging. 21:1280–1291.